Hydrogen-bond structure and dynamics of TADDOL asymmetric organo-catalysts correlate with catalytic activity

Seoncheol Cha, Bogdan Marekha, Manfred Wagner, and Johannes Hunger*

Hydrogen bond structure and dynamics of TADDOL asymmetric organo-catalysts correlate with catalytic activity

Seoncheol Cha,[a] Bogdan Marekha,[a] Manfred Wagner, [a] Johannes Hunger* [a]

[a]*Max Planck Institute for Polymer Research, Ackermannweg 10, 55128 Mainz, Germany*

**email: hunger@mpip-mainz.mpg.de*

SUPPORTING INFORMATION

Diffusion-ordered NMR (DOSY) experiments on 1nTADDOL dissolved in toluene

To exclude intermolecular hydrogen-bond formation of 1nTADDOOL, we perform DOSY experiments at three different concentrations of 1nTADDOL in toluene-d_8. The DOSY spectra in Fig. S1(a) exhibit only two major diffusivities associated to the proton signals of the solvent toluene and of 1nTADDOL. To quantitatively analyse the diffusivities, *D*, we integrate the data from 6.5 ppm to 8.0 ppm to obtain the diffusivities associated with the naphthyl groups of 1nTADDOL and the diffusivities of the aromatic protons of toluene, in Fig. 2(b). The faster component ~ 1 x 10^{-5} cm^2/s agrees well with the diffusion coefficient of toluene and the diffusivity of 1nTADDOL is correspondingly slower ~ 0.5 x 10^{-5} cm^2/s. Upon aggregation of 1nTADDOL the full width at half maximum ($FWHM_{TADDOL}$) of the diffusivity of 1nTADDOL would be expected to increase asymmetrically towards slower values with increasing concentration of 1nTADDOL. As can be seen from Fig. S1 and Table S1, we find no evidence for an increase of $FWHM_{TADDOL}$ with increasing concentration, which renders intermolecular aggregation unlikely. Moreover, we calculated the hydrodynamic radius, *r*, of 1nTADDOL for different concentrations by using Stokes-Einstein relation:

$$r = \frac{k_B T}{6\pi\eta D} \qquad \text{(S1)}$$

where k_B is the Boltzmann constants, *T* the thermodynamic temperature, and η the viscosity of the solution. The viscosities η of TADDOL/toluene mixtures were measured using a rolling-ball viscometer (Anton Paar, Lovis 2000M) at 20 ºC. The increase of the diffusivity of 1nTADDOL parallels the increase of the diffusivity of toluene, which suggests that both diffusion of toluene and 1nTADDOL can be explained by an increase of the solutions' viscosities with increasing concentration of 1nTADDOL. The concentration-independent hydrodynamic radii of 1nTADDOL further supports the absence of intermolecularly bound 1nTADDOL aggregates in the solution.

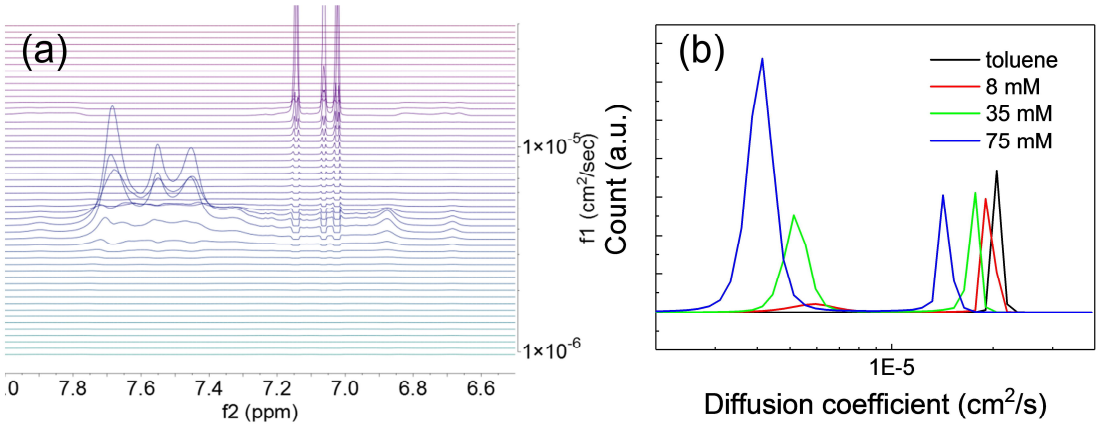

Figure S1. (a) DOSY spectrum of 1nTADDOL dissolved at d_8-toluene at 75 mM concentration. (b) integrated DOSY spectra for neat toluene and 1nTADDOL at 3 different concentrations.

Table S1. Mean diffusivities for toluene, $D_{toluene}$, and TADDOL, D_{TADDOL}, together with the full widths at half maximum $FWHM_j$, obtained by fitting a Gaussian profile to the data in Fig. S1b. $r_{toluene}$ and r_{TADDOL} correspond to the hydrodynamic radii of toluene and TADDOL, respectively, as calculated using eq. S1. η is the solution viscosities.

	$D_{toluene}$ (10^{-5} cm^2/s)	$FWHM_{toluene}$ (10^{-5} cm^2/s)	$r_{tolueene}$ (nm)	D_{TADDOL} (10^{-5} cm^2/s)	$FWHM_{TADDOL}$ (10^{-5} cm^2/s)	r_{TADDOL} (nm)	η (mPa s)
Neat toluene	2.1	0.11	0.18 nm	-	-		0.59[1]
8 mM TADDOL	1.9	0.14	0.17 nm	0.59	0.22	0.54 nm	0.677
38 mM TADDOL	1.5	0.14	0.20 nm	0.52	0.097	0.59 nm	0.714
75 mM TADDOL	1.4	0.13	0.19 nm	0.41	0.084	0.63 nm	0.835

IR spectra of 1nTADDOL in acetone and tetrahydrofuran

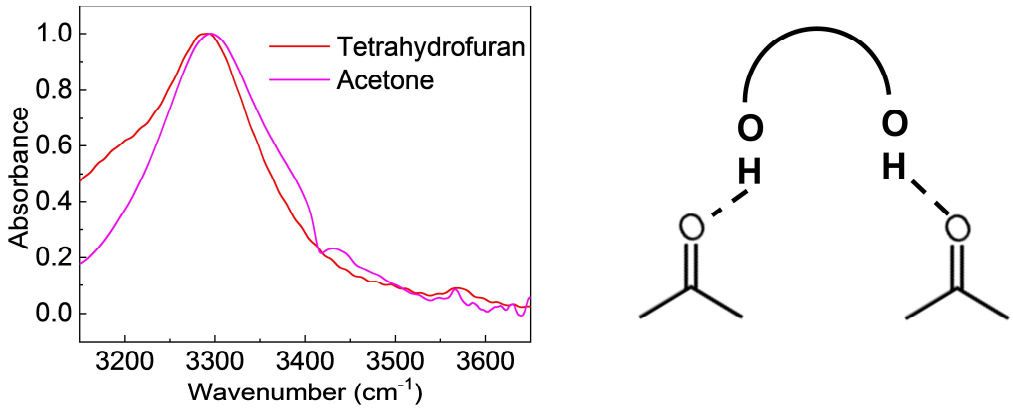

Figure S2. Infrared absorption spectra of 1nTADDOL dissolved in THF and acetone and corresponding molecular hydrogen-bonding scheme.

We note that in hydrogen-bond accepting solvents like tetrahydrofuran (THF) or acetone the bands at >3500 cm^{-1} of 1nTADDOL (see Fig. 4, main manuscript) are completely absent (Fig. S2), similar to what was found for diols interacting with dimethylsulfoxide.[2] In THF and acetone the bound OH bands are even centered at lower wavenumbers than the bound OH band in toluene, which indicates that the intermolecular interaction between TADDOLs OHs and the solvent is stronger than intramolecular hydrogen-bonding.

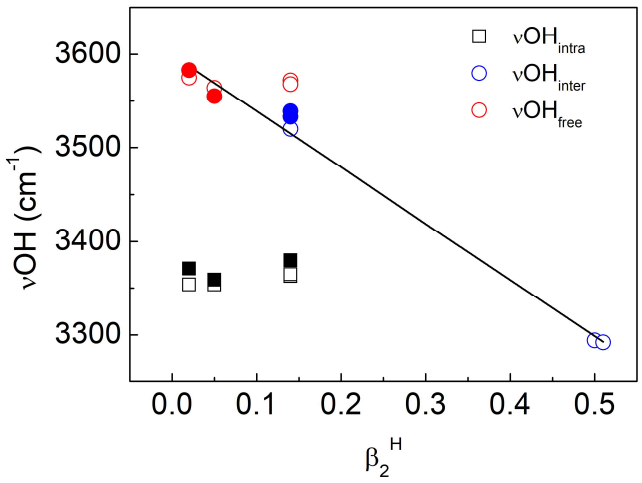

Figure S3. Frequencies of the different νOH bands for 1nTADDOL (open symbols) and 2nTADDOL (filled symbols) as a function of hydrogen-bond acceptor number, β_2^H, of the solvent. νOH_{inter} corresponds to the νOH_π peak in toluene and benzene and to the main peak observed for solutions in THF and acetone. Solid line is a just a visual aid.

In Fig. S3 the peak frequencies of νOH modes of 1nTADDOL and 2nTADDOL are plotted for different solvents versus to the hydrogen-bond accepting (HBA) numbers (β_2^H) of the solvent (β_2^H $CHCl_3$: 0.02, CH_2Cl_2: 0.05 Benzene: 0.14, Toluene: 0.14, Acetone: 0.5, and THF: 0.51).[3] For both TADDOLs we find a linear relation between the OH peak frequency of intermolecularly bonded OH groups and β_2^H.[2] This correlation provides evidence for the 3520 cm^{-1} peak found in aromatic solvents originating from OH-solvent interactions.

Modelling ^{1}H NMR spectrum of 1nTADDOL dissolved in toluene

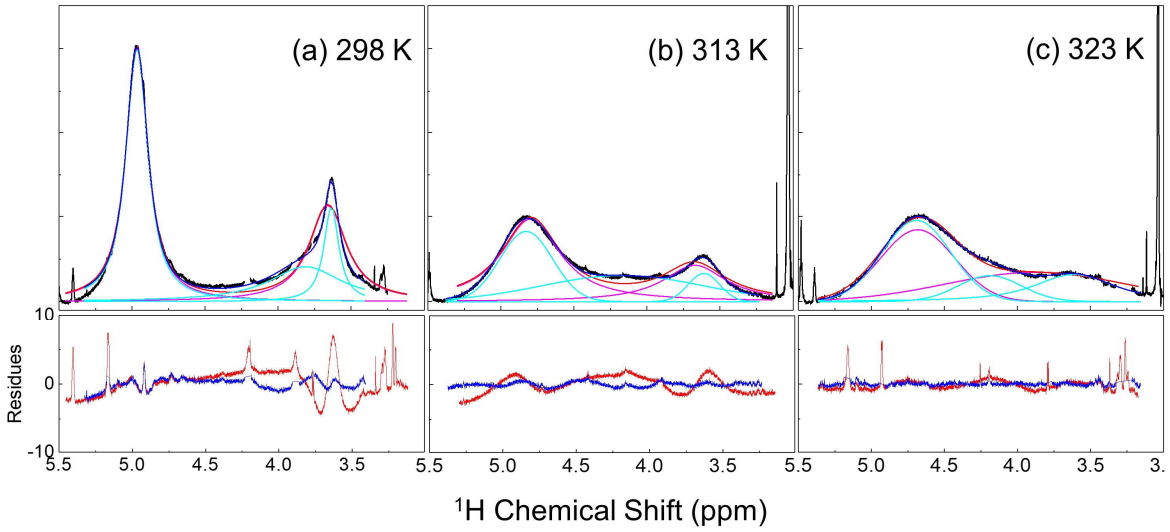

Figure S4. ^{1}H NMR spectra of OH protons (black solid line) of 1nTADDOL dissolved in toluene-d$_8$ at (a) 298 K (b) 313 K (c) 323 K. Red solid lines show the fit using two Voigt peaks and the magenta solid lines show the two individual peaks. Blue solid lines show the fit with three Voigt peaks and the cyan lines their individual contributions to the fit. The bottom panels show the fit residuals for the model consisting of two Voigt functions (red lines) and three Voigt functions (blue lines).

Based on the infrared results and the inferred formation of both free and π-bonded OH groups, we fit the NMR spectra of 1nTADDOL as shown in Fig. S4 using two or three individual peals. The NMR spectra of OH proton regime were decomposed by using a sum of Voigt functions, $S(x)$, which is a convolution of a Gaussian and a Lorenzian distribution:

$$S(x) = A\frac{2ln2}{\pi^{3/2}}\frac{x_L}{x_G^2}\int_{-\infty}^{\infty}\frac{e^{-t^2}}{(\sqrt{ln2})^{x_L}/_{x_G}{}^2+(4\sqrt{ln2}^{x-x_c}/_{x_G}-t)^2}\mathrm{d}t \quad \text{(S2)},$$

where x_L is the Lorenzian and x_G is Gaussian width. x_c is the location of the peak maximum and A the peak amplitude. We use eq. S2 to models both NMR spectra ($x = \delta$) and infrared spectra ($x = \omega$).

Two Voigt functions were used to account for the protons of the intramolecularly bound OH peak at ~ 5 ppm and the free OH peak at ~ 3.6 ppm. The fit residuals (Fig. S4) however improved significantly, when modelling with a sum of three Voigt functions.

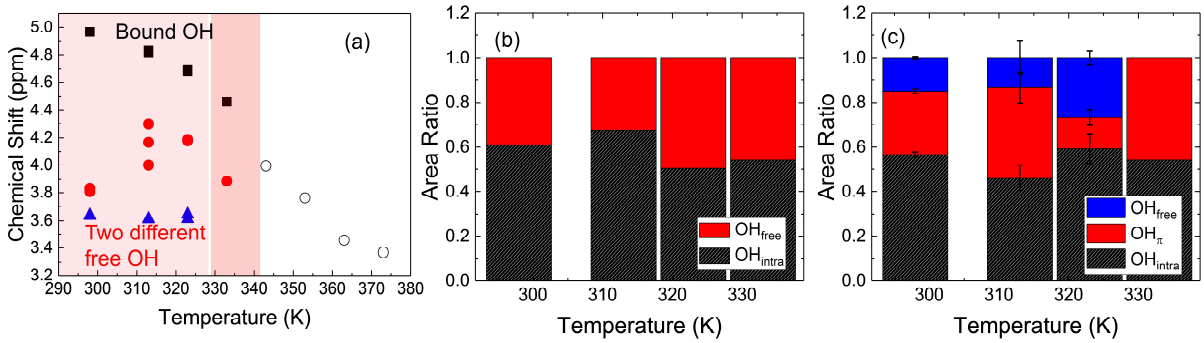

Figure S5. Fit parameters of the fits of the ^{1}H NMR spectra for 1nTADDOL as shown in Fig. S4. (a) Peak maxima (δ_c) using three Voigt functions at temperatures < 330 K and a single Voigt band at temperatures >340 K. At 333 K two Voigt profiles were used to fit the spectra. Also shown are the relative peak areas, A, of the peaks as obtained by (b) two Voigt bands and (c) three Voigt bands for the spectra at temperatures

< 340 K. (black: relative amplitude of bound OH; blue and red areas show the relative amplitude of the free OH and π-OH protons, respectively).

Using three Voigt functions to model the spectra, provides evidence for the three bonding motifs also being discernible in the ^{1}HNMR spectra of 1nTADDOL. In particular, at temperatures below 323 K the three species model provided better description of the experimental spectra. In the three species model, the most down-field shifted proton can be assigned as the bound OH (δOH_{intra}) and two different OH groups at up-field shifted positions at 3.6 ppm and 3.8 ppm at room temperatures. Notably, using three Voigt bands, the ratio of peak areas of (OH_{free} + OH_{π}): (OH_{intra}) is within the experimental error 1:1, in contrast to (OH_{free}): (OH_{intra}) for the fit using two Voigt bands. Above 330 K, it was not required to use multiple peaks as the two- or three different peaks coalesce (Fig. 3 of the main manuscript).

Modelling infrared spectra of 1nTADDOL and 2nTADDOL in toluene

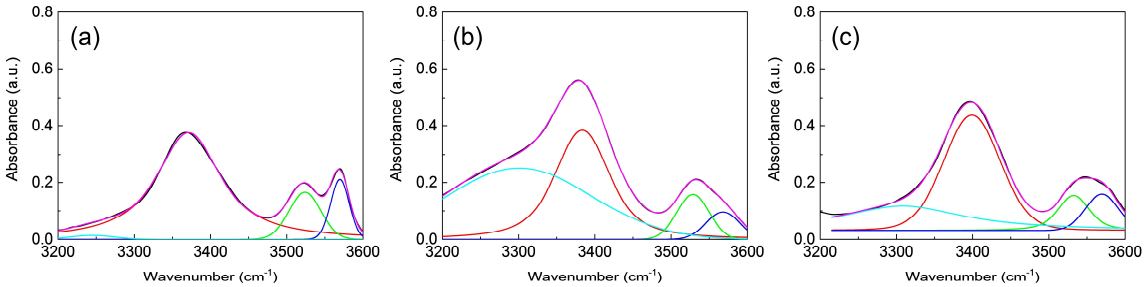

Figure S6. Decomposed infrared spectra of (a) 1nTADDOL at 298 K, (b) 2nTADDOL at 298 K and (c) 2nTADDOL at 368K dissolved in toluene using a combination of four Voigt functions. Black solid lines show the experimental spectrum, cyan, red, green, and blue solid lines show the contributions of the individual Voigt functions. The sum of the four Voigt functions gives the overall fit, which is shown as magenta line.

To quantify the different bonding motifs from the IR spectra, we decompose the spectra using a combination of four Voigt functions (eq. S2): νOH_{intra}, νOH_{π}, νOH_{Free}, and the red-edge absorption of νOH_{intra} ($\nu OH_{intra\text{-}Red}$). For 1nTADDOL at room temperature, the amplitude of $\nu OH_{intra\text{-}Red}$ is rather low, compared to νOH_{intra}. Conversely, the highly asymmetric absorption at ~3400 cm^{-1} for 2nTADDOL cannot be described by a single Voigt functions, and the amplitude of $\nu OH_{intra\text{-}Red}$ is high (Table S1). For 2nTADDOL we also find a higher peak amplitude for νOH_{π} compared to νOH_{Free}, which is not the case for 1nTADDOL. Hence, the peak amplitude $\nu OH_{intra\text{-}Red}$ somewhat correlates with the peak area of νOH_{π}. With increasing temperature from 298 K to 368K, both of the area of $\nu OH_{intra\text{-}Red}$ and νOH_{π} decreased relative to peak areas of νOH_{intra} and νOH_{free}, respectively. Thus, our results suggest that for 2nTADDOL, formation of an OH···π bond also strengthens the intramolecular hydrogen-bond. The strengthening of the intramolecular hydrogen-bond, gives rise to the red-shifted $\nu OH_{intra\text{-}Red}$ band.

Table S2. Parameters obtained by fitting a sum of four Voigt functions to the infrared spectra of 1nTADDOL and 2nTADDOL as shown in Fig. S6.

	Temperature (K)	Peak frequency ω_c (cm^{-1})				Bandwidth ω_G (cm^{-1})				Bandwidth ω_L (cm^{-1})				Relative Peak area			
		intra-Red	intra	π	Free	intra-Red	intra	π	Free	intra-Red	intra	π	Free	intra-Red	intra	π	Free
1nTADDOL	298	3245	3371	3524	3570	71	56	48	28	0	35	1	1	0.01	0.77	0.12	0.09
2nTADDOL	298	3301	3383	3529	3568	224	56	50	51	0	46	0	0	0.51	0.37	0.07	0.04
2nTADDOL	368	3308	3399	3532	3569	0	83	34	50	190	8	48	0	0.33	0.49	0.10	0.09

Infrared spectra of 1nTADDOL-d_2 and 2nTADDOL-d_2 in toluene

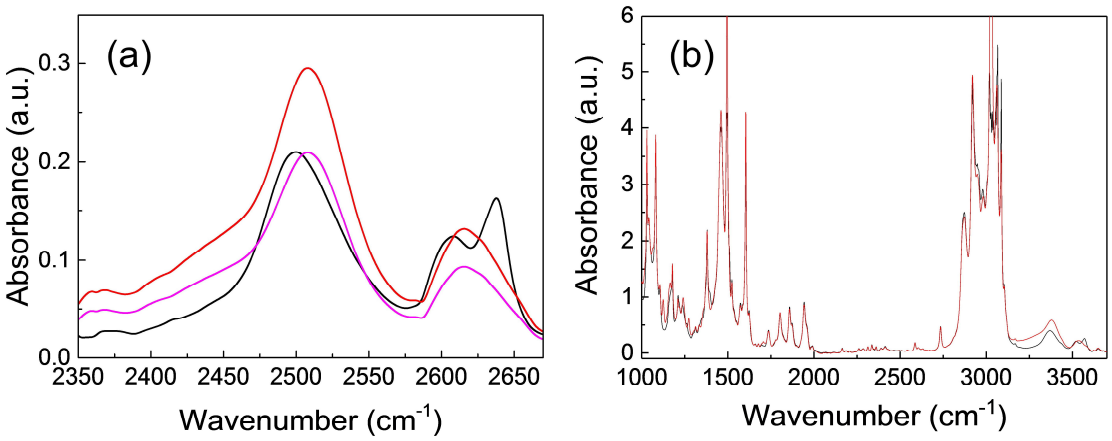

Figure S7. (a) OD stretching absorption for 1nTADDOL-d_2 (black), 2nTADDOL-d_2 (red) and normalized 2nTADDOL-d_2 (magenta). (b) IR spectra of 1nTADDOL (black) and 2nTADDOL (red) at a broad frequency range.

To rule out the possibility of Fermi resonances as the origin of the red-shifted shoulder at ~3250 cm^{-1} of 2nTADDOL (Fig. 5 of the main manuscript), we measured the IR spectra at OD stretching frequencies for isotopically substituted TADDOLs (Fig. S7a). Similar to our results at OH stretching frequencies, the red-shifted shoulder at ~ 2450 cm^{-1} is most pronounced for 2nTADDOL-d_2. The lower frequency spectra nearly collapse onto a single line (Fig. S7b).

Van't Hoff plots to estimate the enthalpy of π-OH bond formation

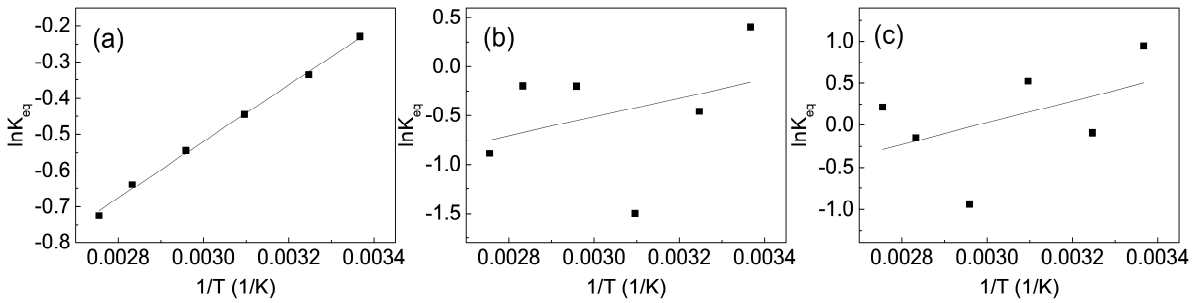

Figure S8. Van't Hoff plot (eq. S3) for (a), (b) 1nTADDOL and (c) 2nTADDOL. The data in (a) are obtained using the absorbance at the frequency of the peak maxima (3520 cm^{-1} for νOH$_\pi$ and 3570 cm^{-1} for νOH$_{free}$) and data in (b) and (c) are obtained by using the decomposition by Voigt functions.

We use the van't Hoff equation to estimate the enthalpy π-OH bond formation:

$$\ln K_{eq} = -\frac{\Delta H}{RT} + \frac{\Delta S}{R} \qquad \text{(S3)}$$

ΔH and ΔS are the enthalpy and entropy of bond formation, respectively, R is the gas constant, and T is the thermodynamic temperature. Values for K_{eq} at different temperatures are determined by the ratio of absorbances of the νOH$_\pi$ and νOH$_{free}$ bands

$$K_{eq} = \frac{A_\pi}{A_{free}} \qquad \text{(S4).}$$

Using the ratio of the absorbance at the peak frequencies (3520 cm^{-1} for νOH$_\pi$ and 3570 cm^{-1} for νOH$_{free}$) to estimate $K_{eq,1nTADDOL}$ (black symbols in Fig. S8a) yields an enthalpy of bond formation of -1.6

kcal/mol. Using the peak absorbance of νOH_{π} and νOH_{free} as obtained from modelling the spectra using Voigt functions (eq. S2, Table S2) to obtain $K_{eq,1nTADDOL}$ (Fig. S8b) gives a very similar enthalpy of bond formation of -1.9 ± 2.5 kcal/mol. $K_{eq,2nTADDOL}$ is thus determined to -2.6 ± 2.4 kcal/mol, which is – within error – similar to $K_{eq,1nTADDOL}$. Because the contribution of the blue-edge of νOH_{bound} significantly affects the amplitude of νOH_{π} (Fig. S6a), the data in Fig. S8b and Fig. S8c are very scattered. Nevertheless, the thus obtained enthalpies are comparable with the formation enthalpy of solvent-solute complexes consisting of alcohols and aromatic solvents ranging from -0.6 kcal/mol to -2.45 kcal/mol obtained by temperature dependent FT-IR measurements and 2D-IR spectroscopy.[4,5] These values are also close to the value estimated from the peak position of the νOH_{π} band, for which simulations for water find the red-shift to correspond to -0.47 kcal/mol hydrogen-bonding enthalpy.[6]

Ab initio calculations for the binding energies of TADDOL-toluene complexes

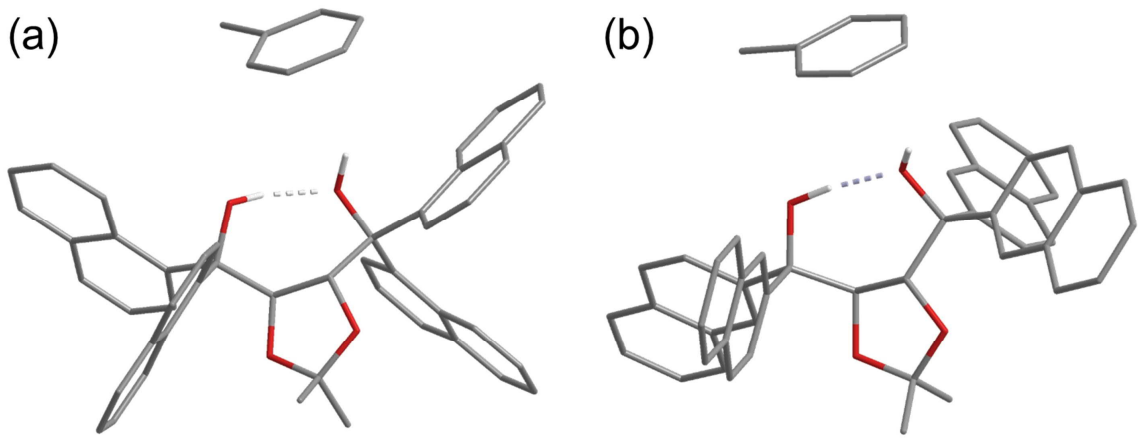

Figure S9. Optimized geometry of (a) 1nTADDOL-toluene and (b) 2nTADDOL-toluene complexes. For visual clarity only protons of OH groups are shown.

To provide further information on the interaction between two different TADDOLs and toluene, we performed *ab initio* calculations for TADDOLs and their complexes with toluene by using the Orca 4.1.1 program package.[7] The geometry optimization is started from the crystal structures of TADDOLs[8,9] using the B3LYP[10]/6-31G*[11] level of theory, similar to previous quantum mechanical studies of TADDOL.[12] The optimized geometries show the T-shaped structure of the bond between intramolecular hydrogen bond accepting OH group and toluene as reported for OH-π hydrogen-bonds.[13] The binding energies for both complexes amount to -3.6 kcal/mol each.

IR absorption of TADDOLs with benzaldehyde

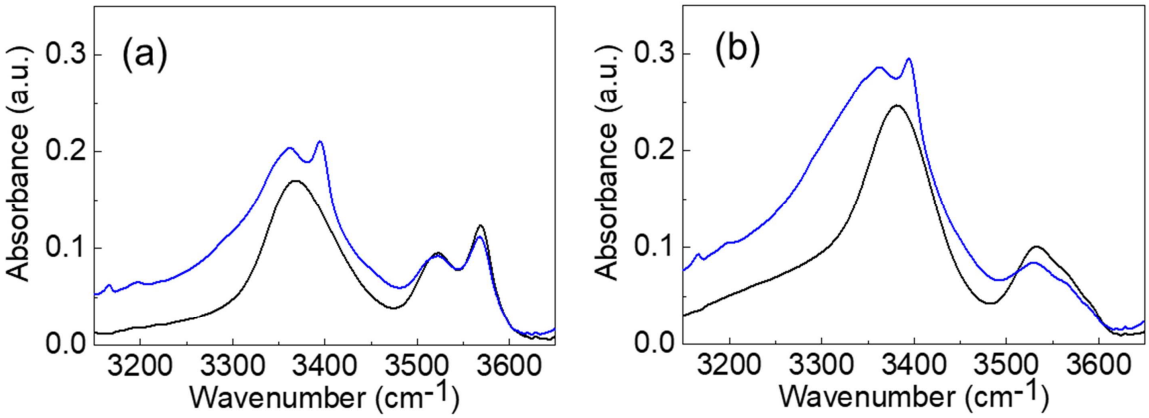

Figure S10. Background subtracted infrared absorption spectra of (a) 1nTADDOL:benzaldehyde and (b) 2nTADDOL:benzaldehyde solutions in toluene (blue lines: 1:10 molar ratio; black lines: 1:0 molar ratio).

To obtain information on the interaction of TADDOLs with typical hydrogen-bond accepting substrates in TADDOL catalysis,[14] we compare the IR absorption spectra of two different TADDOLs with benzaldehyde at the ratio of catalytic condition 1:10. Quantum mechanical studies on TADDOL catalysis predict that the C=O group of benzaldehyde molecule forms intermolecular hydrogen-bonds to the "free OH" groups of TADDOL.[14,15] Consistent with that, the absorptions of νOH_{π} and OH_{free}, decrease for both 1nTADDOL and 2nTADDOL in the presence of benzaldehyde. Notably, the decrement at >3500 cm^{-1} upon addition of benzaldehyde is more pronounced for 2nTADDOL than for 1nTADDOL. Thus, more intermolecular hydrogen-bonds between TADDOL and benzaldehyde are formed for 2nTADDOL compared to 1nTADDOL, similar to our findings for OH···π bonds with toluene. In addition, the absorption of νOH_{intra} is enhanced upon addition of benzaldehyde for both TADDOLs, indicative of the formation of the intermolecular hydrogen-bond between OH groups of TADDOL and C=O groups of benzaldehyde. The clear red-shift of νOH_{intra} of 2nTADDOL also suggests a stronger intermolecular hydrogen-bond between 2nTADDOL and benzaldehyde compared to 1nTADDOL.

Supporting references

[1] D. R. Lide, *CRC Handbook of Chemistry and Physics 87th Edition*, Taylor And Francis Group, **2006**.
[2] M. C. Foti, L. R. C. Barclay, K. U. Ingold, *J. Am. Chem. Soc.* **2002**, *124*, 12881–12888.
[3] M. H. Abraham, P. L. Grellier, D. V. Prior, J. J. Morris, P. J. Taylor, *J. Chem. Soc., Perkin Trans. 2* **1990**, 521–529.
[4] J. Zheng, K. Kwak, X. Chen, J. B. Asbury, M. D. Fayer, *J. Am. Chem. Soc.* **2006**, *128*, 2977–87.
[5] J. Zheng, M. D. Fayer, *J. Am. Chem. Soc.* **2007**, *129*, 4328–4335.
[6] D. Ojha, K. Karhan, T. D. Kühne, *Sci. Rep.* **2018**, *8*, 1–8.
[7] F. Neese, *WIREs Comput. Mol. Sci.* **2012**, *2*, 73–78.
[8] D. Seebach, A. K. Beck, A. Heckel, *Angew. Chem. Int. Ed. Engl.* **2001**, *40*, 92–138.
[9] M. P. L. and S. C. W. C. R. Groom, I. J. Bruno, *Acta. Cryst.* **2016**, *B72*, 171–179.
[10] C. Lee, W. Yang, R. G. Parr, *Phys. Rev. B* **1988**, *37*, 785–789.
[11] W. J. Hehre, R. Ditchfield, J. A. Pople, *J. Chem. Phys.* **1972**, *56*, 2257–2261.
[12] X. Zhang, H. Du, Z. Wang, Y. D. Wu, K. Ding, *J. Org. Chem.* **2006**, *71*, 2862–2869.
[13] K. Kwac, C. Lee, Y. Jung, J. Han, K. Kwak, J. Zheng, M. D. Fayer, M. Cho, *J. Chem. Phys.* **2006**, *125*, DOI 10.1063/1.2403132.
[14] H. Du, D. Zhao, K. Ding, *Chem. - A Eur. J.* **2004**, *10*, 5964–5970.
[15] X. Zhang, H. Du, Z. Wang, Y. Wu, K. Ding, *J. Org. Chem.* **2006**, *71*, 2862–2869.